Article:
Ke, X, Criado, M, Provis, JL et al. (1 more author) (2018) Slag-Based Cements That Resist Damage Induced by Carbon Dioxide. ACS Sustainable Chemistry & Engineering, 6 (4). pp. 5067-5075. ISSN 2168-0485

https://doi.org/10.1021/acssuschemeng.7b04730

A slag-based cement that resists damage induced by carbon dioxide

Xinyuan Ke, Maria Criado, John L. Provis*, Susan A. Bernal*

Department of Materials Science and Engineering, Sir Robert Hadfield Building, The University of Sheffield, Mappin St, Sheffield S1 3JD, United Kingdom

* To whom correspondence should be addressed. Email: s.bernal@sheffield.ac.uk; j.provis@sheffield.ac.uk; phone +44 114 222 5490; fax +44 114 222 5493

Abstract

The use of sodium carbonate as an activator to prepare alkali-activated cements from blast furnace slag and calcined hydrotalcite offers many attractive performance and environmental benefits. However, the understanding of the long-term performance of these cements is limited. In this study, the resistance of sodium carbonate-activated slag cements to carbonation attack was determined under natural (0.04%) and elevated (1.0%) CO_2 concentrations. Two calcium carbonate polymorphs, calcite and vaterite, were formed as carbonation products at a longer time of CO_2 exposure. A cross-linked alkali aluminosilicate gel, and a Ca-deficient calcium (alumino)silicate hydrate gel were identified to form by decalcification of the main binding phases initially present in these cements. However, despite these carbonation-induced mineralogical changes, the mechanical strength after carbonation was comparable to that of non-carbonated specimens, which is contrary to previous observations of strength loss due to carbonation of slag-rich cements. The high carbonation resistance of sodium carbonate-activated slag cement indicates these materials have the potential to resist attack by atmospheric CO_2 in service with sustained mechanical performance.

Keywords: Alkali-activated cements, carbonation, calcium carbonate, durability, layered double hydroxides.

Introduction

The cement industry is facing the challenge of reducing its environmental footprint while dealing with a continuously increasing demand for this essential material. This has motivated the development of non-Portland cements, including alkali-activated cements (AACs), which are prepared using the powders that are normally blended with Portland cement (PC) as supplementary cementitious materials (e.g. blast furnace slags, fly ashes, calcined clays, and others) together with an alkali activator which enables them to generate cementing character and high mechanical performance without the addition of Portland clinker [1-2]. In many aspects AACs develop performance which is comparable to that of blended Portland-based cements [2-3].

The selection of the alkali source used as the activator strongly influences the microstructural features and the physico-mechanical performance of an AAC [4-6], as well as the environmental impacts associated with its production [7-9]. The most commonly used activators include sodium hydroxide and sodium silicate. A recent life cycle analysis of AACs revealed that although these cements have much lower global warming potentials than PC, the use of sodium hydroxide and/or sodium silicate as activators brings a higher environmental impact in aspects including human toxicity, fresh water and marine ecotoxicity [9]. The industrial production of sodium silicate is also an energy intensive process, and the commonly used furnace process requires reacting sodium carbonate (Na_2CO_3) and sand (SiO_2) at 1100-1200 °C [10]. To replace sodium silicate with sodium carbonate, as an alternative alkali-activator, has the potential to greatly reduce the environmental impact of alkali-activated cements, especially in regions where there are abundant geological resources of sodium carbonate that can be mined from trona deposits [11]. The sodium carbonate produced from natural deposits is now around a quarter of the global production,[12] and this process leads to significantly lower greenhouse gas emissions than the industrial synthesis of sodium carbonate by the Solvay process [13].

It is well known that alkali-activation of blast furnace slag to form cements is achievable using mild alkaline solutions based on sodium carbonate [2, 4, 14-17]. However, earlier attempts using sodium carbonate as the sole activator were barely satisfactory in terms of use in modern engineering and construction practice, as prolonged setting times (up to 1-5 days at

ambient temperature) were observed, followed by slow development of strength [3, 18-19]. Recent studies have elucidated that the consumption of carbonate anions supplied by the activator dominates the early kinetics of reaction of these cements [17]. In particular, the formation of a layered double hydroxide hydrotalcite-like phase ($[Mg_{1-x}Al_x(OH)_2]^{x+}[OH,CO_3]_{x/m}\cdot nH_2O$, $0.20<x<0.33$, m: charge of anion and n: hydration number), in parallel with other carbonate-containing phases, plays a key role in chemically binding the carbonate present in the pore solution [20] and can be tailored to promote fast hardening. Incorporation of a small fraction of a calcined mineral addition designed to favor the formation of this phase (specifically, a calcined layered double hydroxide, CLDH) into these cements can greatly enhance this effect. The addition of this CLDH also promotes good mechanical performance, and reduces chloride permeability compared with sodium silicate-activated AAC, or with Portland cement [20-21].

The carbonation of cement hydrate products is one of the main degradation mechanisms of cements and concretes, and involves a chemical reaction between the alkaline binder and the CO_2 present in the atmosphere. Thus, significant attention is paid to this process when assessing the durability performance of concrete structures in many exposure conditions, as it can induce a reduction of the pH within the concrete and consequently increase the probability of corrosion of steel reinforcement [22-24]. However, the carbonation of cements in service has also been identified as a large potential carbon sink [22, 25], before reaching the point that the carbonation-induced degradation would jeopardize the safety performance of the structure. In Portland cement, the presence of portlandite ($Ca(OH)_2$) provides a buffer phase, consuming atmospheric CO_2 as it is converted to calcium carbonate. This delays the decalcification process of the main strength-giving phase, a calcium silicate hydrate [26]. However, in AACs, the absence of portlandite and the high alkalinity of the pore solution have made carbonation one of the main durability-related concerns [27-28]. For the specific case of sodium carbonate-activated slag cement, the information available from the literature regarding its resistance to carbonation is very limited. However, it has been observed that after exposure to atmosphere conditions for over 35 years, sodium carbonate-activated slag concrete presented an increased strength [29], suggesting that the carbonation process taking place in these cement most likely differs from that in sodium silicate-activated slag cements, which tends to lose strength as a result of carbonation [30-31]. Hence, the development of a new fundamental understanding of the structural changes induced by carbonation of sodium

carbonate-activated slag cement is crucial, not only for assessment of its durability performance, but also for evaluation of its whole-service-life carbon footprint.

Therefore, in this study, the structural stability of sodium carbonate-activated slag cements upon exposure to natural and high CO_2 concentrations was determined, as well as the effects of its chemical modification via the addition of a calcined layered double hydroxide, as a potential CO_2 binding agent.

Experimental Program

Materials

A commercial ground granulated blast furnace slag was used in this study, a glassy material mainly consisting of CaO (41.3 wt.%), SiO_2 (36.0 wt.%), Al_2O_3 (11.3 wt.%), and MgO (6.5 wt.%). This slag had a Blaine fineness of 5056 ± 22 cm^2/g (average value of four measurements), and an average particle size d_{50} of 11.2 ± 0.1 μm (determined using laser diffraction).

The activator was prepared by pre-dissolving commercial sodium carbonate powder (Sigma Aldrich, $Na_2CO_3 \geq 99.5\%$) into distilled water. A calcined layered double hydroxide (CLDH) was produced by thermally treating synthetic hydrotalcite (Sigma Aldrich) at 500°C, following the procedure described in a previous study [20], where detailed characterization of the synthetic hydrotalcite, before and after treatment, was reported.

Sample preparation

Sodium carbonate-activated slag pastes were produced with an activator dose of 8 g Na_2CO_3 per 100 g slag, and a water/(slag+Na_2CO_3) mass ratio of 0.40. To some of the pastes, 5 wt.% CLDH (by mass of anhydrous slag) was also added. Pastes were mixed using an overhead mixer with a high-shear blade, cast in centrifuge tubes, then sealed and stored at room temperature (20 ± 3 °C) until testing. Sodium carbonate-activated slag mortars were also prepared with a sand to slag mass ratio of 3:1, where BS EN 196-1 standard sand [32] was used, and cured under the same conditions as the pastes.

Test methods

Slag paste samples that had been cured for 28 and 180 days were crushed and sieved to a particle size of between 100 μm and 250 μm, exposed to atmospheric carbonation (~0.04% CO_2, described as *naturally carbonated*), and elevated carbonation condition (1.0 ± 0.2% CO_2, described as *accelerated carbonated*). Under both carbonation conditions, the temperature and relative humidity was controlled at 20 ± 2 ºC and 65 ± 5%, respectively. The accelerated carbonation conditions were selected based on a previous study [28] where it was demonstrated that alkali-activated samples carbonated under these conditions develop comparable carbonation reaction products to those forming after several years of atmospheric exposure. Pastes exposed to both CO_2 conditions for up to 14 days were analyzed. Reference samples sealed in centrifuge tubes and kept under the same laboratory conditions (20 ± 2 ºC, described as *non-carbonated*) were analyzed at similar times to those used for carbonation, to account for the structural evolution taking place in these cements as they continued to mature during the period of CO_2 exposure. Specimens were analyzed through:

- X-ray diffraction (XRD), using a Bruker D2 Phaser instrument with Cu-Kα radiation and a nickel filter. The tests were conducted with a step size of 0.02° and a counting time of 1 s/step, from 5° to 55° 2θ.
- Thermogravimetry-mass spectroscopy (TG-MS), in a Perkin Elmer TGA 4000 instrument coupled with a Hiden mass spectrometer. In each case, 30 mg of sample was tested from 30°C to 1000°C at a heating rate of 3°C/min, under nitrogen flowing at 40 mL/min.
- Solid-state ^{29}Si MAS NMR spectra were collected at 79.4 MHz on a Varian VNMRS 400 (9.4 T) spectrometer, using a probe for 6.0 mm outer diameter zirconia rotors, and a spinning speed of 6 kHz. The ^{29}Si MAS NMR spectra were collected with a 90° pulse duration of 4.6 μs, a recycle delay of 5 s, and between 6000 and 17000 repetitions. The solid state ^{27}Al MAS NMR spectra were acquired on the same spectrometer at 104.20 MHz, using a probe for 4 mm outer diameter zirconia rotors, a spinning speed of 14 kHz with a pulse duration of 1 μs (approximately 25°), a recycle delay of 0.2 s, and a minimum of 7000 repetitions. ^{29}Si and ^{27}Al chemical shifts are referenced to external samples of neat tetramethylsilane (TMS) and a 1.0 M aqueous solution of $Al(NO_3)_3$, respectively.

Mortar cubes with dimensions of 50×50 mm were used for testing compressive strength, which was determined using an automatic testing machine (Controls Automax5) with a loading speed of 0.25 MPa/s. Triplicate samples were measured per curing condition at each time point. The carbonation penetration depth after exposure of mortar cubes to natural and accelerated carbonation was also determined, using a spray of 1 wt.% phenolphthalein indicator solution (dissolving 1.0 g of phenolphthalein in 50 mL of ethanol and then adding 50 mL of water) onto a freshly split surface as an indicator.

Results and discussion

Formation of $CaCO_3$ polymorphs

In accordance with previous evaluation of the phase evolution of sodium carbonate-activated slag cement [20], the main reaction products identified by XRD analysis of the three non-carbonated samples assessed (0 wt.% CLDH after 28 and 180 days and 5 wt.% CLDH after 28 days, Figure 1) were semi-crystalline (Al, Na)-substituted calcium silicate hydrate (C-(N)-A-S-H) type gel (crystal structure close to PDF #00-019-0052), and layered double hydroxide phases including both hydrotalcite-structured and AFm-structured (hydrocalumite-like) phases. Specifically, the AFm phases identified by XRD were hemicarboaluminate (PDF #00-036-0129) and monocarboaluminate (PDF #00-036-0377). Hemicarboaluminate is often observed in low MgO-content samples (< 5 wt.% within the slag) at lower degree of reaction (i.e. early age), while monocarboaluminate is often observed in samples with moderate MgO content at later age [20]. Gaylussite (PDF #00-021-0343) is normally identified in sodium carbonate-activated slag pastes at early age as a transient phase [20], consistent with its identification here only in the 28-day samples without CLDH addition in Figure 1. The 180-day samples, and the 28-day samples with 5% CLDH addition, have higher content of hydrotalcite-like phases (PDF #00-014-0525) than the 28-day sample without CLDH addition.

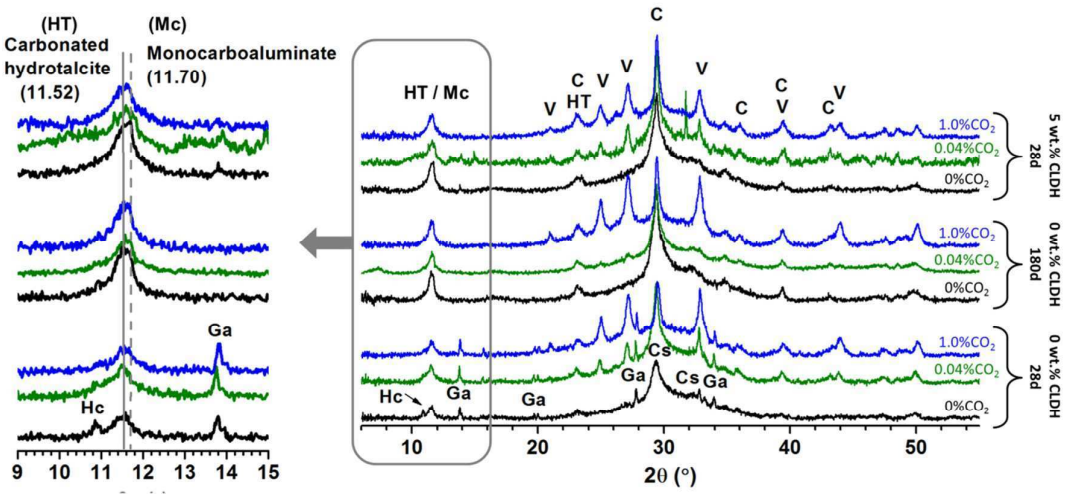

Figure 1. X-ray diffraction patterns of the sodium carbonate-activated slag pastes, after being exposed to 0% (non-carbonated), 0.04% (naturally carbonated) and 1.0% CO_2 (accelerated carbonated) for 24 hours. Phases marked are: Cs - calcium (sodium) aluminate silicate hydrate; C - calcite, V - vaterite; HT - hydrotalcite-like phase; Ga - gaylussite; Hc - hemicarboaluminate, Mc – monocarboaluminate. The inset on the left enlarges the low-angle region.

When the pastes were exposed to CO_2, there was a significant increase in the content of two polymorphs of $CaCO_3$: calcite (PDF# 00-005-0586) and vaterite (PDF# 00-033-0268), as a result of the decalcification of the C-(N)-A-S-H type gel [28] (Figure 1). The gaylussite present in the 28-day sample without CLDH did not seem to be influenced by carbonation, while the small fraction of hemicarboaluminate in the same sample seemed to have been carbonated to monocarboaluminate. A higher amount of both $CaCO_3$ polymorphs was formed under exposure to more aggressive carbonation concentrations, indicating a higher content of decalcification of the main reaction product, as observed in sodium silicate-activated slag cements [28, 33]. The same trend has been observed in samples exposed to a more extended time of carbonation (see Supporting Information). At a higher extent of carbonation, whether achieved by increasing the CO_2 concentration and/or by extending the exposure time, the formation of vaterite seems to be favored over calcite. The precipitation of $CaCO_3$ polymorphs is known to be closely related to the activities of Ca^{2+} and CO_3^{2-}, as well as pH and concentrations of other dissolved ions in the aqueous phase [34-36]. The pH values at which different $CaCO_3$ polymorphs precipitate are different, and the addition of alkali (e.g. NaOH) could inhibit the precipitation of well-crystallized calcite [36]. When the carbonation process in an alkali-activated cement starts, the atmospheric CO_2 gradually dissolves in the alkaline pore solution (pH>13), consumes OH^-, and leads to an increased concentration of CO_3^{2-} in the

pore solution [37]. The decreased alkalinity of the pore solution destabilizes the C-(N)-A-S-H type gel, and results in increased Ca^{2+} concentration in the carbonated pore solution [37-38]. The increased concentration of both Ca^{2+} and CO_3^{2-} in the pore solution, together with decreased pH, favors the formation of vaterite over calcite [35].

The samples cured for 180 days without CLDH addition appear to have the lowest amount of calcium carbonate forming, suggesting the highest carbonation resistance under natural carbonation conditions, likely due to the presence of higher amount of dense, space-filling hydrous reaction product phases at extended times of curing [20]. Samples modified with 5 wt.% CLDH have higher hydrotalcite-group phase content, which enables them to absorb additional CO_2 by its incorporation via substitution of hydroxide in these phases [39-40]. Figure 2 demonstrates this additional CO_2 binding in the CLDH-containing sample by TG-MS: compared with the paste without CLDH modification (blue line, Figure 2), the CLDH-modified sample (orange line, Figure 2) showed a significantly higher mass loss centered at around 373 °C caused by the release of CO_2, consistent with that which is observed from carbonated hydrotalcite-like phases [41]. Additionally, the mass loss from these two samples (blue and orange lines, Figure 2) below 200 °C, associated with the water loss from the main reaction product C-(N)-A-S-H type gel, appeared to be similar. These observations may indicate that the addition of CLDH enables the binder to take up a higher content of CO_2 without damaging the main strength-giving reaction product phases.

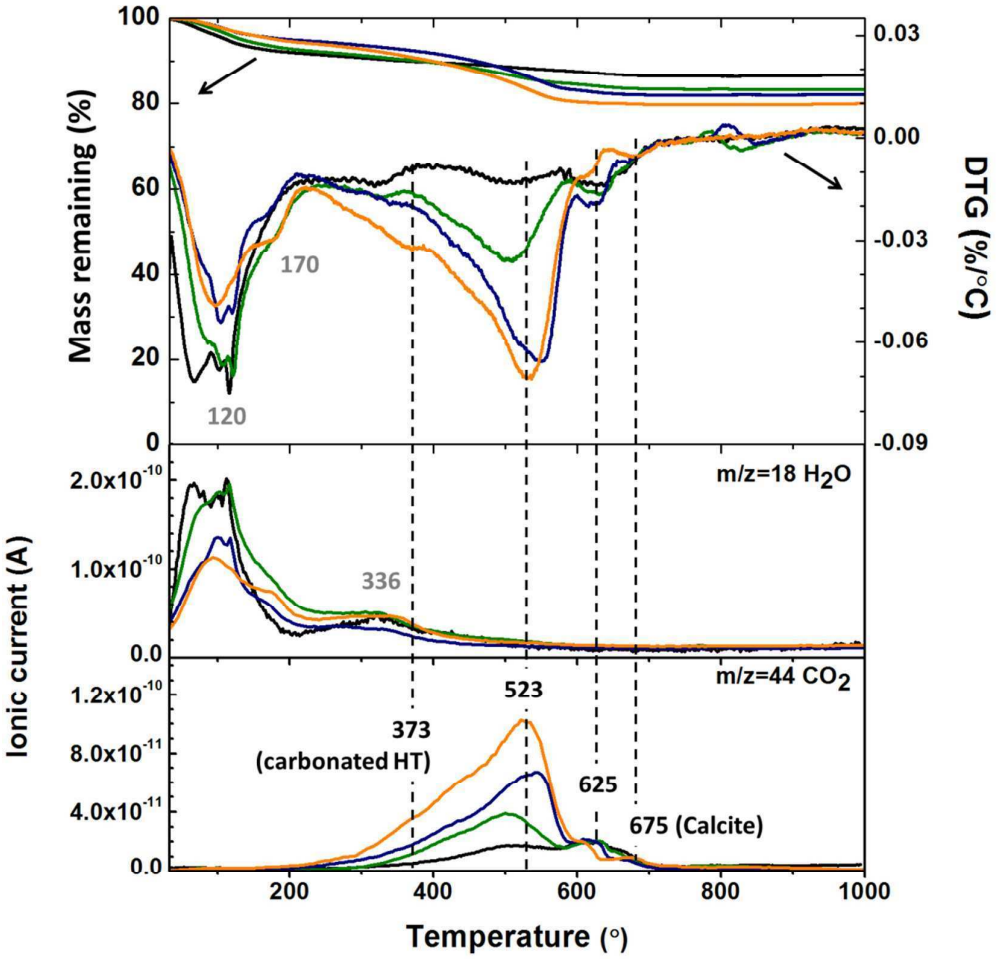

Figure 2. TG-MS data for sodium carbonate-activated slag paste (28d, 0 wt.% CLDH) exposed to 0% (black line), 0.04% (green line) and 1.0% CO_2 (blue line) for 24 hours, and a CLDH modified sample (28d, 5 wt.% CLDH) exposed to 1.0% CO_2 for 24 hours (orange line)

As calcium carbonate salts form upon carbonation in sodium carbonate-activated slags, their formation requires the release of calcium from the C-(N)-A-S-H type gels. So, the long term stability of these materials will depend on the structural changes that take place in these strength-giving phases [28], and the changes in microstructure that may alter the pore volume and connectivity [31]. These factors therefore need further investigation, as discussed in the following sections.

Structural changes in calcium aluminosilicate hydrate type gels

The main reaction product in these cements is a sodium-rich calcium aluminosilicate hydrate (C-(N)-A-S-H) type gel, which has a disordered tobermorite-like structure consisting of dreierketten silicate chain units, and with some of the Si sites substituted by Al [42-43]. Solid-state ^{29}Si and ^{27}Al magic angle spinning nuclear magnetic resonance (MAS NMR) spectroscopy provides valuable information to identify changes in the coordination environments of Si and Al atoms within this gel, as a consequence of carbonation.

In the ^{29}Si MAS NMR spectra (Figure 3), three distinct resonance at -79 ppm, -82 ppm and -85 ppm were identified in non-carbonated slag pastes with or without CLDH after 28 and 180 days of curing; these are assigned to Q^1, $Q^2(1Al)$ and Q^2 sites within the C-(N)-A-S-H type gel [44]. The broad resonance centered at -74 ppm is attributed to the fraction of unreacted slag, mainly consisting of Q^0 and some Q^1 and Q^2 sites (Figure 3D). The assignments of these silica sites were chosen in accordance with the previous study of Ke et al. [20], where samples of corresponding composition were prepared and characterized. After 24 hours of exposure to natural carbonation (green lines in Figure 3), decreased intensity of the Q^1 and $Q^2(1Al)$ sites, along with an increase in the intensity of the Q^2 resonance, were observed. Samples exposed to 1.0% CO_2 for 24 hours underwent much more significant structural changes as a result of exposure to this higher CO_2 concentration (blue lines). A significant decrease in all chain-type silicate environments was observed, while an intense but broad band centered at around -95 ppm appeared. The chemical shift of this site correlates with crosslink-type silica sites (Q^3) or tetrahedral silica coordinated in part by Al (most likely $Q^4(2Al)$) [45].

Comparing the ^{29}Si MAS NMR spectra of the various samples exposed to 0.04% CO_2 for 24 hours (Figure 3), it appears that the decalcification process starts with the loss of interlayer Ca, that was initially charge balancing either end-chain Q^1 site or $Q^2(1Al)$ sites. This enables the un-balanced silica sites to bridge with the neighboring un-balanced silica sites, thus increasing the content of crosslinked or network silica sites (i.e. Q^3 or Q^4). These mechanisms are consistent with the observed increase in connectivity of the C-(N)-A-S-H type gel after

carbonation, similar to that which is identified in C-S-H type gels [46], which decompose to a crosslinked silica gel plus calcium carbonate under similar exposure conditions.

The loss of the chain-like structure of the C-(N)-A-S-H gel upon carbonation, particularly at high CO_2 concentrations (1.0% CO_2), is also similar to the behavior observed in carbonated sodium silicate [28, 38, 40] and sodium hydroxide-activated slag pastes [38], where the continuous loss of Q^1 and Q^2 silica sites is associated with a higher extent of carbonation. It appears that the C-(N)-A-S-H type gel in the sodium carbonate activated slag paste cured for 180 days prior to carbonation was more stable than the gels which formed in either of the 28-day cured samples (Figure 3, with or without CLDH), consistent with observations from XRD (Figure 1, and Supporting Information). However, the addition of CLDH did not seem to have significantly altered the residual C-(N)-A-S-H structure formed upon carbonation (comparing Figure 3A and C), although there was more CO_2 absorbed in the binder (Figure 2).

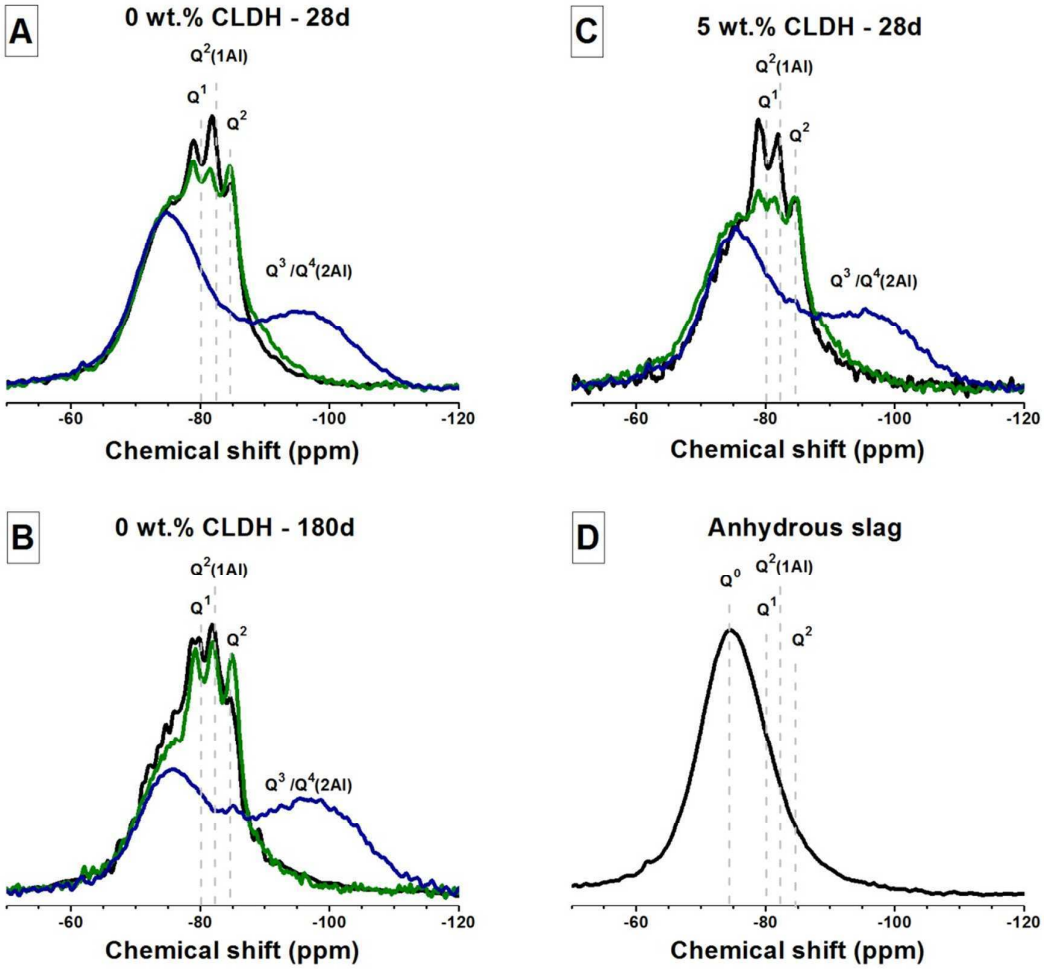

Figure 3. ^{29}Si MAS NMR spectra of sodium carbonate-activated slag pastes exposed to 0% (black line), 0.04% (green line) and 1.0% CO_2 (blue line) for 24 hours. Results for non-carbonated samples are from [20].

Two distinct Al environments were identified from the ^{27}Al MAS NMR results in Figure 4. The resonance at around 60-80 ppm corresponds to $Al^{[IV]}$ and is assigned to the tetrahedral Al environments in C-(N)-A-S-H type gel (also partially contributed by unreacted slag), and the $Al^{[VI]}$ resonances at chemical shift values below 20 ppm are assigned to the Al sites in the two types of LDH structures present (Mg-Al and AFm) [44-45]. The chemical shift of tetrahedrally-coordinated Al decreases at a higher degree of crosslinking. The ^{27}Al MAS NMR resonance of $Al^{[IV]}$ in chain-type aluminosilicates normally appears at between 70 ppm to 80 ppm, while in tetrahedral framework aluminosilicates this peak appears at between 55 to 68 ppm [45]. The shift of the $Al^{[IV]}$ peak in Figure 4 therefore suggests the release of $Al^{[IV]}$ from C-(N)-A-S-H type gel, and formation of a more highly cross-linked aluminosilicate type gel. Correlating this result with the observation of the ^{29}Si MAS NMR spectra in Figure 3, the

broad chemical shift of $Al^{[IV]}$ centered at around 60 ppm in samples exposed to 0.04% CO_2 is likely to be contributed mainly by Al in cross-linked C-(N)-A-S-H type gel, as only a small fraction of highly crosslinked Si sites were formed. However, for samples exposed to 1.0% CO_2, where a large fraction of cross-linked Si sites was identified, the intense and narrow band centered at 56 ppm (Figure 4) identified in all samples indicates the presence of $Al^{[IV]}$ in Q^4 sites with largely similar coordination environments, similar to that identified in sodium-aluminosilicate geopolymers [47-48].

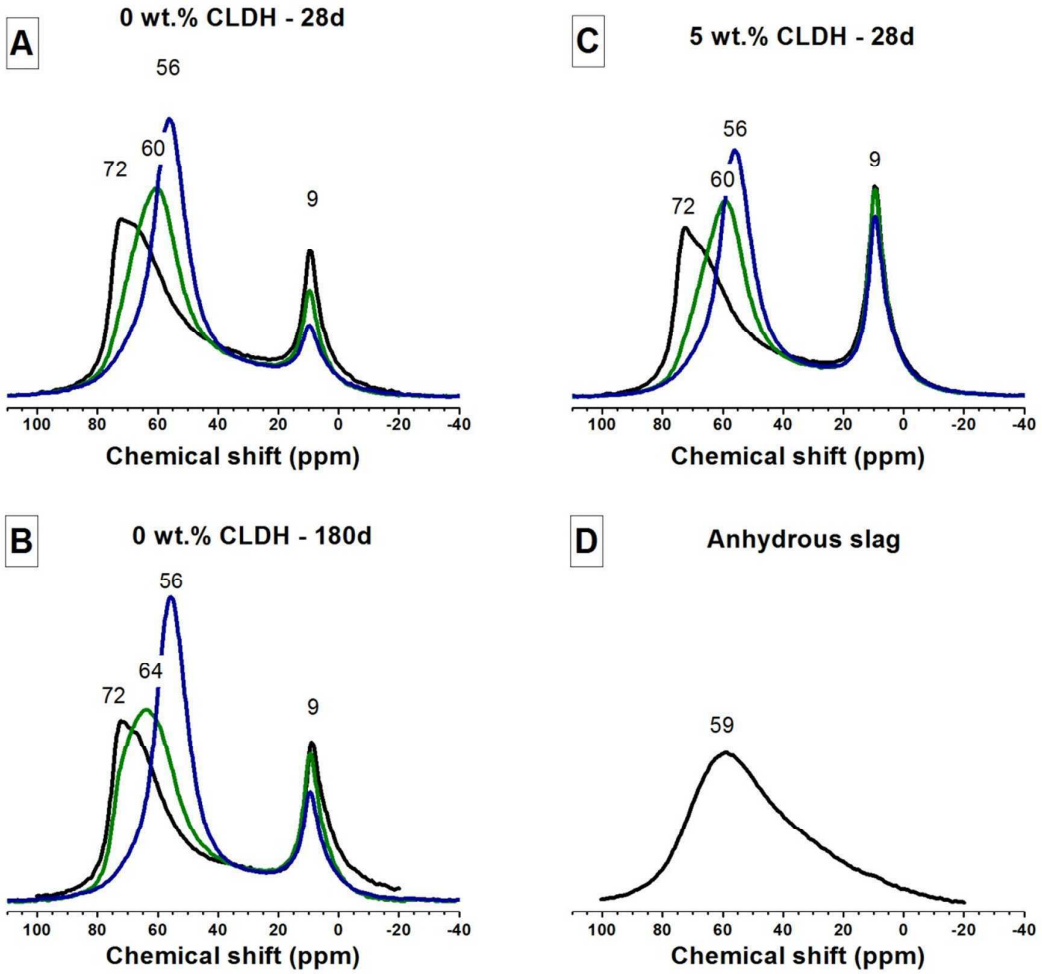

Figure 4. ^{27}Al MAS NMR spectra of sodium carbonate-activated slag pastes (curing conditions as marked), exposed to 0% (black line), 0.04% (green line) and 1.0% CO_2 (blue line) for 24 hours, and the spectrum of the unreacted slag. Results for non-carbonated samples are from [20].

The decrease in the relative intensities of the $Al^{[VI]}$ band at 9 ppm in Figure 4 as a result of carbonation is caused by the decomposition of AFm phases at the lower pH induced by carbonation [49-50], in agreement with the disappearance of AFm phases from the XRD data in Figure 1 after carbonation. The alumina released from the decomposed AFm phase might also become incorporated into the highly cross-linked aluminosilicate gel. In comparison, the hydrotalcite-like Mg-Al LDH is much more stable when exposed to carbonation, and so samples with 5% CLDH showed the least decrease in the $Al^{[VI]}$ band.

Some fraction of the unreacted slag may also react with CO_2 during the carbonation process. However, this process has been observed to take place very slowly unless under high temperature and high CO_2 pressure [51], or in an aqueous solution preferably with higher alkalinity [52-53]. In AACs, the carbonation reaction would be expected to start from the gel binder phases between the slag grains first, and it would require a long time of exposure before having a significant influence on the unreacted slag grains [33]. Therefore, the main structural changes should be considered to take place in the gel binder phases.

A proposed scheme of structural changes in sodium carbonate activated slag paste during the carbonation process is illustrated in Figure 5.

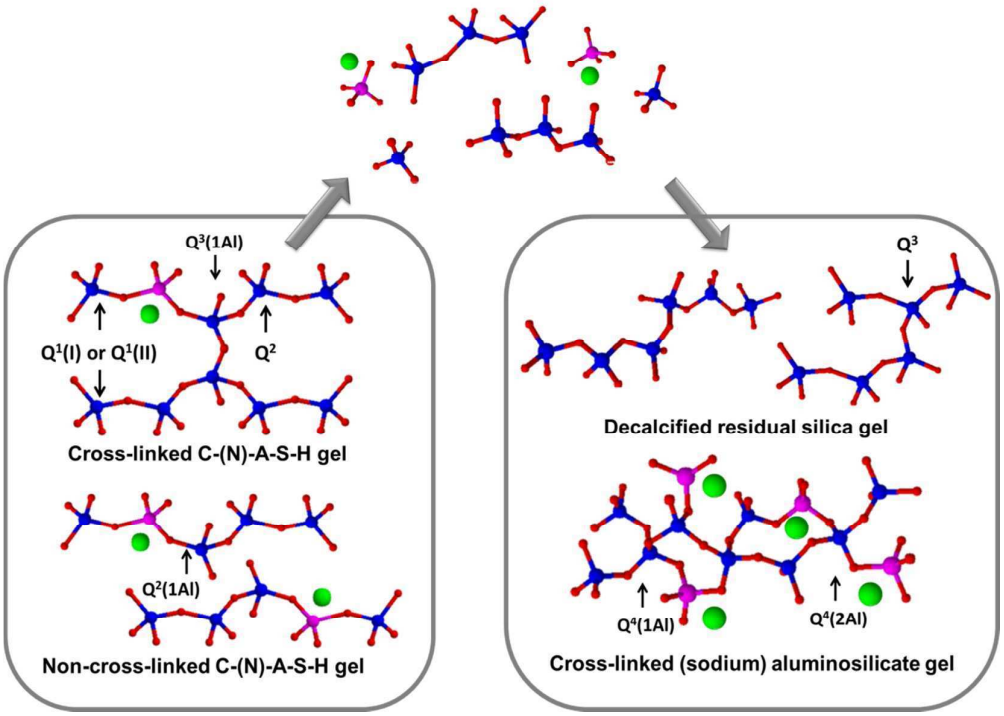

Figure 5. Structural changes in sodium carbonate activated slag paste during carbonation, where the blue balls represent Si, the pink balls represent Al, the red balls represent O, and the green balls represent Na.

The potential for effective carbon sequestration

If carbonation of these cements is to be considered as a useful carbon sink, an essential prerequisite is that there is not a loss of performance (strength or durability-related characteristics) as a result of this process. Figure 6 shows the changes in compressive strength of mortar cubes cured for 28 days and exposed to different carbonation conditions. The increase in the strength of non-carbonated (0% CO_2) samples was contributed by the increased degree of slag reaction over time [21]. In comparison, samples exposed to natural carbonation conditions (0.04% CO_2) exhibited essentially the same strength evolution, at the low extent of carbonation reached. For samples exposed to accelerated carbonation conditions (1% CO_2), the compressive strength remained relatively constant at the level reached after 28 days of sealed curing, and the greater carbonation depth indicated a much higher extent of carbonation. Samples with 5% CLDH showed very similar strength performance to these 0% CLDH samples at the longest carbonation exposure time measured (see Supporting Information, Figure S4). The higher compressive strengths of 5% CLDH

samples at early age were induced by the influence of CLDH [21], which does not seem to influence long-term strength performance under carbonation.

As explained previously, the adoption of accelerated testing conditions was intended to simulate years of CO_2 exposure under a natural atmosphere; therefore the lower compressive strength obtained from the samples after accelerated carbonation might not occur even after years of ambient exposure. The continuing development of strength as a result of the ongoingly increasing degree of reaction of the cement under natural carbonation conditions would also be expected to densify the cementitious matrix over the years, making it less permeable to the carbon dioxide.

The strength evolution of sodium carbonate activated slag mortar upon carbonation is opposite to that observed in sodium silicate-activated slag mortars, where the compressive strength has been observed to decrease significantly with increased carbonation depth as the result of increased pore volumes [54]. However in the sodium carbonate-activated system, the overall intrudable porosity decreased after carbonation (see Supporting Information for MIP results), suggesting that the precipitation of calcium carbonates might have blocked the connected pores, similar to carbonation behaviors that have been reported for PC [55].

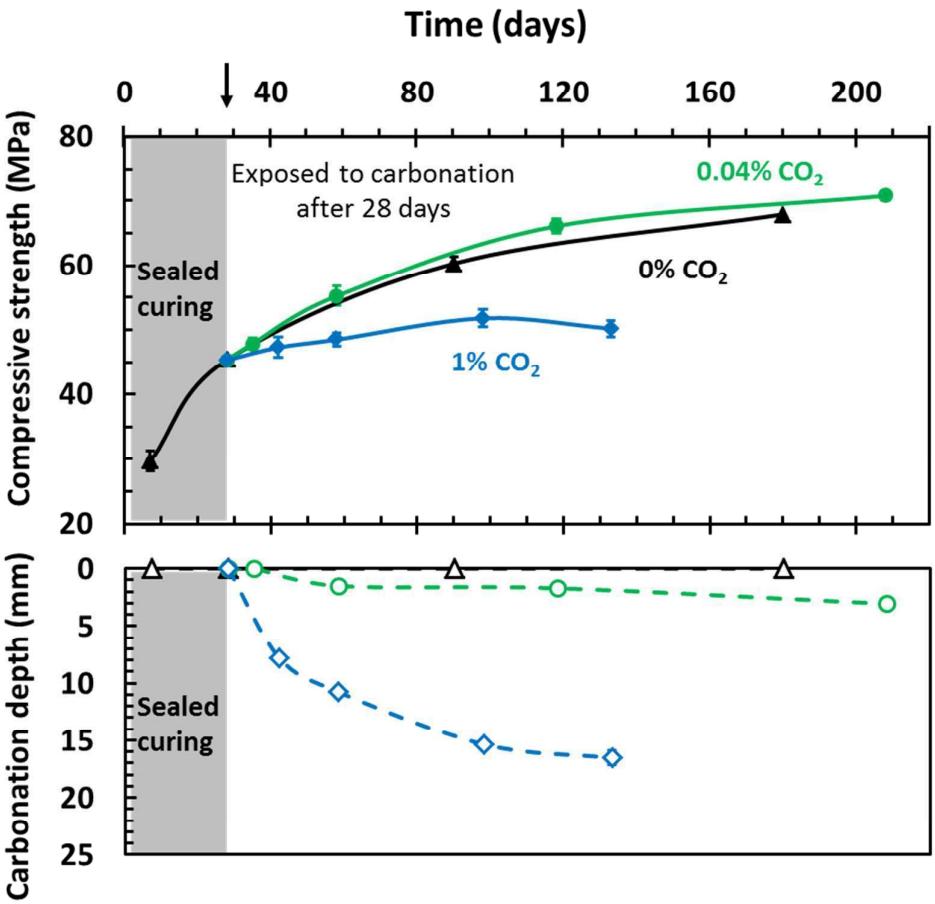

Figure 6. Changes in compressive strength of sodium carbonate activated slag mortar and corresponding carbonation depths, after exposure to different carbonation conditions. All samples were cured for 28 days in sealed plastic bags before carbonation exposure.

It has previously been shown that alkali-activated binders subjected to natural carbonation are able to retain sufficient alkalinity that steel corrosion is not necessarily going to be initiated, even once the carbonation front has passed the steel-concrete interface [56-58]. The total carbon uptake of a cementitious material during its life cycle accumulates with time, where a longer service life is normally associated with higher CO_2 uptake [25]. The degradation in mechanical strength that normally takes place in in sodium silicate-activated slag cement upon carbonation [30-31] was not observed in sodium carbonate-activated slag cements, suggesting that the sodium carbonate-activated slag cement could have a longer service life under atmospheric carbonation conditions without degradation in its performance, while taking up a modest quantity of CO_2 (Figure 3) into its structure and giving some degree of carbon sequestration.

Conclusions

Carbonation of sodium carbonate-activated slag cements under natural and accelerated conditions results in both the formation of calcium carbonate (as both vaterite and calcite polymorphs), and structural changes in the strength-giving cement hydrate phases. An assemblage of decalcified C-S-H type gel and cross-linked alkali aluminosilicate gel were formed as a result of decalcification of the C-(N)-A-S-H type gel which is the main binding phase in these cements. The incorporation of a calcined hydrotalcite-like layered double hydroxide (CLDH) increases the capacity for uptake of CO_2 into these binders in service, without bringing changes to the structures of the main reaction products. Unlike some other alkali-activated slag cements, which have been described in the literature, the sodium carbonate-activated slag cements investigated here maintain their mechanical strength upon carbonation.

Acknowledgments

This research was funded by the European Research Council under the European Union's Seventh Framework Programme (FP7/2007-2013) / ERC Grant Agreement #335928 (GeopolyConc). The participation of SAB in this research was partially funded by the UK Engineering and Physical Sciences Research Council (EPSRC) through grant EP/M003272/1. Solid-state NMR spectra were obtained at the EPSRC UK National Solid-state NMR Service at Durham. The technical support provided by Dr. Oday H. Hussein is also greatly acknowledged.

Supporting Information

The following contents are provided as Supporting Information:

- XRD patterns of the phase evolution of three samples assessed as a function of CO_2 concentration (0.04 % and 1.0 %), and exposure time (from 4 hours up to 14 days);
- Compressive strength of sodium carbonate activated slag mortars (with 5% CLDH, sealed for 28 days) after exposure to different carbonation conditions
- Differential pore volume distributions in carbonated mortar fractions measured using MIP

References

1. Juenger, M. C. G.; Winnefeld, F.; Provis, J. L.; Ideker, J. H., Advances in alternative cementitious binders. *Cem. Concr. Res.* **2011,** *41*, 1232-1243. DOI 10.1016/j.cemconres.2010.11.012

2. Provis, J. L.; Bernal, S. A., Geopolymers and related alkali-activated materials. *Annu. Rev. Mater. Res.* **2014,** *44*, 299-327. DOI 10.1146/annurev-matsci-070813-113515

3. Bernal, S. A.; Provis, J. L.; Fernández-Jiménez, A.; Krivenko, P. V.; Kavalerova, E.; Palacios, M.; Shi, C., Binder chemistry–high-calcium alkali-activated materials. In: *Alkali-Activated Materials, State of the Art Report of RILEM TC 224-AAM*, Dordrecht, Springer: 2014; pp 59-91. DOI 10.1007/978-94-007-7672-2_3

4. Fernández-Jiménez, A.; Puertas, F., Setting of alkali-activated slag cement. Influence of activator nature. *Adv. Cem. Res.* **2001,** *13*, 115-121. DOI 10.1680/adcr.2001.13.3.11

5. Bernal, S. A.; San Nicolas, R.; van Deventer, J. S. J.; Provis, J. L., Alkali-activated slag cements produced with a blended sodium carbonate/silicate activator. *Adv. Cem. Res.* **2015,** *28*, 262-273. DOI 10.1680/jadcr.15.00013

6. Duran Atiş, C.; Bilim, C.; Çelik, Ö.; Karahan, O., Influence of activator on the strength and drying shrinkage of alkali-activated slag mortar. *Constr. Build. Mater.* **2009,** *23*, 548-555. DOI 10.1016/j.conbuildmat.2007.10.011

7. Provis, J. L., Green concrete or red herring? – future of alkali-activated materials. *Adv. Appl. Ceram.* **2014,** *113*, 472-477. DOI 10.1179/1743676114Y.0000000177

8. Habert, G.; d'Espinose de Lacaillerie, J. B.; Roussel, N., An environmental evaluation of geopolymer based concrete production: reviewing current research trends. *J. Cleaner Prod.* **2011,** *19*, 1229-1238. DOI 10.1016/j.jclepro.2011.03.012

9. Habert, G.; Ouellet-Plamondon, C., Recent update on the environmental impact of geopolymers. *RILEM Techn. Lett.* **2016,** *1*, 17-23. DOI 10.21809/rilemtechlett.2016.6

10. Fawer, M.; Concannon, M.; Rieber, W., Life cycle inventories for the production of sodium silicates. *Int. J. Life Cycle Assessment* **1999,** *4*, 207-212. DOI 10.1007/bf02979498

11. Sharma, B. K., *Industrial Chemistry*. GOEL Publishing House, Delhi: 1991.

12. Kostick, D. S. *2011 Minerals Yearbook*; U.S. Department of the Interior, U.S. Geological Survey, Washington DC: 2012.

13. Office of Air and Radiation, Technical support document for the soda ash manufacturing sector: proposed rule for mandatory reporting of greenhouse gases. United States EPA, Washington DC, 2009.

14. Bai, Y.; Collier, N.; Milestone, N.; Yang, C., The potential for using slags activated with near neutral salts as immobilisation matrices for nuclear wastes containing reactive metals. *J. Nucl. Mater.* **2011,** *413*, 183-192. DOI 10.1016/j.jnucmat.2011.04.011

15. Escalante-García, J. I.; Fuentes, A. F.; Gorokhovsky, A.; Fraire-Luna, P. E.; Mendoza-Suarez, G., Hydration products and reactivity of blast-furnace slag activated by various alkalis. *J. Am. Ceram. Soc.* **2003,** *86*, 2148-2153. DOI 10.1111/j.1151-2916.2003.tb03623.x

16. Glukhovsky, V. D.; Krivenko, P. V.; Rostovskaya, G. S.; Timkovich, V. J.; Pankratov, V. L., Binder. United States Patent 4,410,365, 1983.

17. Bernal, S. A.; Provis, J. L.; Myers, R. J.; San Nicolas, R.; van Deventer, J. S. J., Role of carbonates in the chemical evolution of sodium carbonate-activated slag binders. *Mater. Struct.* **2014,** *48*, 517-529. DOI 10.1617/s11527-014-0412-6

18. Wang, S.-D.; Scrivener, K. L.; Pratt, P. L., Factors affecting the strength of alkali-activated slag. *Cem. Concr. Res.* **1994,** *24*, 1033-1043. DOI 10.1016/0008-8846(94)90026-4

19. Fernández-Jiménez, A.; Puertas, F., Effect of activator mix on the hydration and strength behaviour of alkali-activated slag cements. *Adv. Cem. Res.* **2003,** *15*, 129-136. DOI 10.1680/adcr.2003.15.3.129

20. Ke, X.; Bernal, S. A.; Provis, J. L., Controlling the reaction kinetics of sodium carbonate-activated slag cements using calcined layered double hydroxides. *Cem. Concr. Res.* **2016,** *81*, 24-37. DOI 10.1016/j.cemconres.2015.11.012

21. Ke, X.; Bernal, S. A.; Hussein, O. H.; Provis, J. L., Chloride binding and mobility in sodium carbonate-activated slag pastes and mortars. *Mater. Struct.* **2017,** *50*, #252. DOI 10.1617/s11527-017-1121-8

22. Fernández-Bertos, M.; Simons, S. J. R.; Hills, C. D.; Carey, P. J., A review of accelerated carbonation technology in the treatment of cement-based materials and sequestration of CO_2. *J. Hazard. Mater.* **2004,** *B112*, 193-205. DOI 10.1016/j.jhazmat.2004.04.019

23. Sanjuán, M. A.; Andrade, C.; Cheyrezy, M., Concrete carbonation test in natural and accelerated conditions. *Adv. Cem. Res.* **2003,** *15*, 171 - 180. DOI 10.1680/adcr.2003.15.4.171

24. Hobbs, D. W., Concrete deterioration: causes, diagnosis, and minimising risk. *Int. Mater. Rev.* **2001,** *46*, 117-144. DOI 10.1179/095066001101528420

25. Xi, F.; Davis, S. J.; Ciais, P.; Crawford-Brown, D.; Guan, D.; Pade, C.; Shi, T.; Syddall, M.; Lv, J.; Ji, L.; Bing, L.; Wang, J.; Wei, W.; Yang, K.-H.; Lagerblad, B.; Galan, I.; Andrade, C.; Zhang, Y.; Liu, Z., Substantial global carbon uptake by cement carbonation. *Nat. Geosci.* **2016,** *9*, 880-883. DOI 10.1038/ngeo2840

26. Taylor, H. F. W., *Cement Chemistry*. Thomas Telford, London: 1997.

27. Puertas, F.; Fernández-Jiménez, A.; Blanco-Varela, M. T., Pore solution in alkali-activated slag cement pastes. Relation to the composition and structure of calcium silicate hydrate. *Cem. Concr. Res.* **2004,** *34*, 139-148. DOI 10.1016/S0008-8846(03)00254-0

28. Bernal, S. A.; Provis, J. L.; Walkley, B.; San Nicolas, R.; Gehman, J. D.; Brice, D. G.; Kilcullen, A. R.; Duxson, P.; van Deventer, J. S. J., Gel nanostructure in alkali-activated binders based on slag and fly ash, and effects of accelerated carbonation. *Cem. Concr. Res.* **2013,** *53*, 127-144. DOI 10.1016/j.cemconres.2013.06.007

29. Xu, H.; Provis, J. L.; van Deventer, J. S. J.; Krivenko, P. V., Characterization of aged slag concretes. *ACI Mater. J.* **2008,** *105*, 131-139. DOI 10.14359/19753

30. Bernal, S. A.; Mejía de Gutierrez, R.; Provis, J. L.; Rose, V., Effect of silicate modulus and metakaolin incorporation on the carbonation of alkali silicate-activated slags. *Cem. Concr. Res.* **2010,** *40*, 898-907. DOI 10.1016/j.cemconres.2010.02.003

31. Puertas, F.; Palacios, M.; Vázquez, T., Carbonation process of alkali-activated slag mortars. *J. Mater. Sci.* **2006,** *41*, 3071-3082. DOI 10.1007/s10853-005-1821-2

32. British Standards Institute, BS EN 196-1:2005 Methods of testing cement. Part 1: Determination of strength, London, UK, 2005.

33. Bernal, S. A.; San Nicolas, R.; Provis, J. L.; Mejía de Gutiérrez, R.; van Deventer, J. S. J., Natural carbonation of aged alkali-activated slag concretes. *Mater. Struct.* **2014,** *47*, 693-707. DOI 10.1617/s11527-013-0089-2

34. Jun, K.; Norimasa, S.; Akira, M.; Masao, K., Precipitation diagram of calcium carbonate polymorphs: its construction and significance. *J. Phys.: Condens. Matter* **2009,** *21*, 425102. DOI 10.1088/0953-8984/21/42/425102

35. Han, Y. S.; Hadiko, G.; Fuji, M.; Takahashi, M., Crystallization and transformation of vaterite at controlled pH. *J. Cryst. Growth* **2006,** *289*, 269-274. DOI 10.1016/j.jcrysgro.2005.11.011

36. Gal, J.-Y.; Bollinger, J.-C.; Tolosa, H.; Gache, N., Calcium carbonate solubility: a reappraisal of scale formation and inhibition. *Talanta* **1996,** *43*, 1497-1509. DOI 10.1016/0039-9140(96)01925-X

37. Bernal, S. A.; Provis, J. L.; Brice, D. G.; Kilcullen, A.; Duxson, P.; van Deventer, J. S. J., Accelerated carbonation testing of alkali-activated binders significantly underestimates service life: The role of pore solution chemistry. *Cem. Concr. Res.* **2012,** *42*, 1317-1326. DOI 10.1016/j.cemconres.2012.07.002

38. Palacios, M.; Puertas, F., Effect of carbonation on alkali-activated slag paste. *J. Am. Ceram. Soc.* **2006,** *89*, 3211-3221. DOI 10.1111/j.1551-2916.2006.01214.x

39. Dadwhal, M.; Kim, T. W.; Sahimi, M.; Tsotsis, T. T., Study of CO_2 diffusion and adsorption on calcined layered double hydroxides: the effect of particle size. *Ind. Eng. Chem. Res.* **2008,** *47*, 6150-6157. DOI 10.1021/ie701701d

40. Bernal, S. A.; San Nicolas, R.; Myers, R. J.; Mejía de Gutiérrez, R.; Puertas, F.; van Deventer, J. S. J.; Provis, J. L., MgO content of slag controls phase evolution and structural changes induced by accelerated carbonation in alkali-activated binders. *Cem. Concr. Res.* **2014,** *57*, 33-43. DOI 10.1016/j.cemconres.2013.12.003

41. Ke, X.; Bernal, S. A.; Provis, J. L., Uptake of chloride and carbonate by Mg-Al and Ca-Al layered double hydroxides in simulated pore solutions of alkali-activated slag cement. *Cem. Concr. Res.* **2017,** *100*, 1-13. DOI 10.1016/j.cemconres.2017.05.015

42. Faucon, P.; Delagrave, A.; Richet, C.; Marchand, J. M.; Zanni, H., Aluminum incorporation in calcium silicate hydrates (C−S−H) depending on their Ca/Si ratio. *J. Phys. Chem. B* **1999,** *103*, 7796-7802. DOI 10.1021/jp990609q

43. Richardson, I. G.; Brough, A. R.; Groves, G. W.; Dobson, C. M., The characterization of hardened alkali-activated blast-furnace slag pastes and the nature of the calcium silicate hydrate (C-S-H) phase. *Cem. Concr. Res.* **1994,** *24*, 813-829. DOI 10.1016/0008-8846(94)90002-7

44. Wang, S.-D.; Scrivener, K. L., ^{29}Si and ^{27}Al NMR study of alkali-activated slag. *Cem. Concr. Res.* **2003,** *33*, 769-774. DOI 10.1016/S0008-8846(02)01044-X

45. Engelhardt, G.; Michel, D., *High-Resolution Solid-State NMR of Silicates and Zeolites*. John Wiley & Sons: Chichester, 1987.

46. Sevelsted, T. F.; Skibsted, J., Carbonation of C–S–H and C–A–S–H samples studied by ^{13}C, ^{27}Al and ^{29}Si MAS NMR spectroscopy. *Cem. Concr. Res.* **2015,** *71*, 56-65. DOI 10.1016/j.cemconres.2015.01.019

47. Melar, J.; Renaudin, G.; Leroux, F.; Hardy-Dessources, A.; Nedelec, J.-M.; Taviot-Gueho, C.; Petit, E.; Steins, P.; Poulesquen, A.; Frizon, F., The porous network and its interface inside geopolymers as a function of alkali cation and aging. *J. Phys. Chem. C* **2015,** *119*, 17619-17632. DOI 10.1021/acs.jpcc.5b02340

48. Duxson, P.; Provis, J. L.; Lukey, G. C.; Separovic, F.; van Deventer, J. S. J., ^{29}Si NMR study of structural ordering in aluminosilicate geopolymer gels. *Langmuir* **2005,** *21*, 3028-3036. DOI 10.1021/la047336x

49. Runcevski, T.; Dinnebier, R. E.; Magdysyuk, O. V.; Pollmann, H., Crystal structures of calcium hemicarboaluminate and carbonated calcium hemicarboaluminate from synchrotron powder diffraction data. *Acta Crystallogr. B* **2012,** *68*, 493-500. DOI 10.1107/S010876811203042X

50. Mesbah, A.; Cau-dit-Coumes, C.; Renaudin, G.; Frizon, F.; Leroux, F., Uptake of chloride and carbonate ions by calcium monosulfoaluminate hydrate. *Cem. Concr. Res.* **2012,** *42*, 1157-1165. DOI 10.1016/j.cemconres.2012.05.012

51. Yu, J.; Wang, K., Study on characteristics of steel slag for CO_2 capture. *Energy & Fuels* **2011,** *25*, 5483-5492. DOI 10.1021/ef2004255

52. Huijgen, W. J. J.; Comans, R. N. J., Carbonation of steel slag for CO_2 sequestration: leaching of products and reaction mechanisms. *Environ. Sci. Technol.* **2006,** *40*, 2790-2796. DOI 10.1021/es052534b

53. Kasina, M.; Kowalski, P. R.; Michalik, M., Mineral carbonation of metallurgical slags. *Mineralogia*, **2015**, *45*, 27-45. DOI 10.1515/mipo-2015-0002

54. Bernal, S. A.; Mejía de Gutiérrez, R.; Provis, J. L., Engineering and durability properties of concretes based on alkali-activated granulated blast furnace slag/metakaolin blends. *Constr. Build. Mater.* **2012,** *33*, 99-108. DOI 10.1016/j.conbuildmat.2012.01.017

55. Tuutti, K., *Corrosion of steel in concrete*. Kungliga Tekniska Högskolan i Stockholm: CBI Forskning 82:4, 1982.

56. Pouhet, R.; Cyr, M., Carbonation in the pore solution of metakaolin-based geopolymer. *Cem. Concr. Res.* **2016,** *88*, 227-235. DOI 10.1016/j.cemconres.2016.05.008

57. Badar, M. S.; Kupwade-Patil, K.; Bernal, S. A.; Provis, J. L.; Allouche, E. N., Corrosion of steel bars induced by accelerated carbonation in low and high calcium fly ash geopolymer concretes. *Constr. Build. Mater.* **2014,** *61*, 79-89. DOI 10.1016/j.conbuildmat.2014.03.015

58. Mundra, S.; Criado, M.; Bernal, S. A.; Provis, J. L., Chloride-induced corrosion of steel rebars in simulated pore solutions of alkali-activated concretes. *Cem. Concr. Res.* **2017,** *100*, 385-397. DOI 10.1016/j.cemconres.2017.08.006

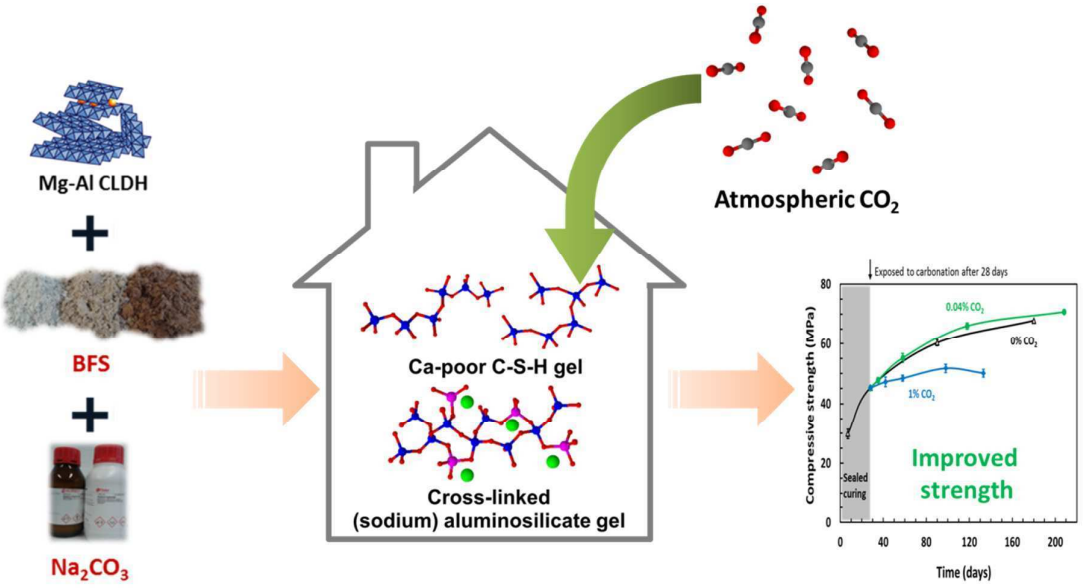

Graphical abstract: a chemically modified slag-based cement that retains its strength after carbon dioxide exposure.